Theor Chem Acc (2010) 127:627–639
DOI 10.1007/s00214-010-0762-2

REGULAR ARTICLE

Theoretical studies on the hydration of formic acid by ab initio and ABEEM$\sigma\pi$ fluctuating charge model

Shu-Ling Chen · Dong-Xia Zhao · Li-Dong Gong · Zhong-Zhi Yang

Received: 9 March 2010 / Accepted: 3 May 2010 / Published online: 27 May 2010

Abstract The interaction between formic acid (FA) and water was systemically investigated by atom-bond electronegativity equalization method fused into molecular mechanics (ABEEM$\sigma\pi$/MM) and ab initio methods. The geometries of 20 formic acid–water complexes (FA–water) were obtained using B3LYP/aug-cc-pVTZ level optimizations, and the energies were determined at the MP2/aug-cc-pVTZ level with basis set superposition error (BSSE) and zero-point vibrational energy (ZPVE) corrections. The ABEEM$\sigma\pi$ potential model gives reasonable properties of these clusters when compared with the present ab initio data. For interaction energies, the root mean square deviation is 0.74 kcal/mol, and the linear coefficient reaches 0.993. Next, FA in aqueous solution was also studied. The hydrogen-bonding pattern due to the interactions with water has been analyzed in detail. Furthermore, the ABEEM$\sigma\pi$ charges changed when H_2O interacted with the FA molecule, especially at the sites where the hydrogen bonds form. These results show that the ABEEM$\sigma\pi$ fluctuating charge model is fine giving the overall characteristic hydration properties of FA–water systems in good agreement with the high-level ab initio calculations.

Keywords ABEEM$\sigma\pi$ fluctuating charge model · Ab initio calculation · Hydrogen bond · Formic acid–water complex

1 Introduction

Formic acid (FA) is a major organic constituent in cloud and fogwater, as well as in precipitation, and FA is one of the simplest organic molecules and has been often considered as a model for studying the biological systems exhibiting the organic acidic type of bonding [1]. The driving forces for the formation of atmospheric molecular complexes are hydrogen-bonding interactions, and atmospherically relevant hydrogen-bonding complexes have been the subject of numerous theoretical studies in recent years [2–6]. The nature of hydrogen bonds between FA and water can explain the hydrogen-bonding mechanism expected in the hydration of organic acids. A significant amount of FA in the atmosphere is present in the aqueous phase. Although previous studies have examined complexes of water and FA using both theoretical and experimental methods [7–14], here we do systematic studies on this system both in the gas phase and in the aqueous phase by the ABEEM$\sigma\pi$ fluctuating charge model.

The FA molecule has a Cs symmetry, and its flexibility is limited to the torsional motion of the hydroxy group around the C–OH bond. Several chemicophysical properties of FA depend on its capability to form different types

Electronic supplementary material The online version of this article (doi:10.1007/s00214-010-0762-2) contains supplementary material, which is available to authorized users.

S.-L. Chen · D.-X. Zhao · L.-D. Gong · Z.-Z. Yang (✉)
School of Chemistry and Chemical Engineering,
Liaoning Normal University, 116029 Dalian,
People's Republic of China
e-mail: zzyang@lnnu.edu.cn

S.-L. Chen
e-mail: wk_csl@163.com

D.-X. Zhao
e-mail: zhaodx@lnnu.edu.cn

L.-D. Gong
e-mail: gongjw@lnnu.edu.cn

of hydrogen bonds (H-bond). A FA molecule can actually act both as hydrogen-bond acceptors/donors with the two oxygen atoms, and as hydrogen donors with the hydroxy and formyl hydrogen atoms. The major types of intermolecular hydrogen bonds that occur in FA–water complexes are C=O···Hw, H–O···Hw and O–H···Ow, respectively. These special types of nonbonded interactions have been studied by various ab initio [11, 15–17] and density functional quantum chemical methods [7, 12, 13], and the calculations at different levels have been carried out for FA–water systems to investigate intermolecular interactions, and yield theoretical structures and other static properties. The geometry optimization of the FA water clusters has been carried out using SCF, MP2, and B3LYP [18] correlation methods with the 6-31g, 6-31g(d), 6-31+g(d), 6-311++g(d,p), and 6-311++g(2d,2p) basis sets, along with analytic vibrational frequency calculations have been discussed in paper [11, 12]. DFT and MP2 levels of theory with the large basis sets give similar results as far as the geometrical and vibrational features of FA–water complexes and their monomers are concerned in their paper. Hence, the DFT [19, 20] method has been adopted as an excellent compromise between computational cost and accuracy. The Pople type basis sets [21], such as 6-31G, 6-311G, etc., and the Dunning correlation consistent basis sets [22], such as aug-cc-pVDZ, aug-cc-PVTZ [22, 23], etc., are widely used. A careful study of the effect of basis set and level of theory on the calculated geometries of a series of small molecules having one or two non-hydrogen atoms has been reported by Helgaker et al. [24]. They found that aug-cc-pVTZ gave quite good results.

In addition, in order to fit the parameters of the molecular mechanics force field MM4 [25], the calculations for the acids, esters and acid dimer systems were performed at the B3LYP/6-311++G(2d,2p) level. Other molecular mechanics force field such as MM3 [26], MMFF [27], CHARMM [28], and AMBER [29] have done some research of this system. The crucial problem in these force fields arises from the calculation of Coulomb interactions with the fixed charges that neglect all mutual polarizations and charge-transfer effects. There has been steady interest since the 1970s in the development and use of polarizable force fields [30]. Furthermore, some electrostatic protocols including polarization effects have been widely developed in the past few years. The first application of the fluctuating charge model to water system and the aqueous solvation of amides were reported by Rick et al. [31, 32]. These models are called TIP4P-FQ and SPC-FQ, using the TIP4P and SPC water geometries. Lately, Yang et al. [33] reported a new water model: a transferable, intermolecular, seven-point approach including fluctuation charges and flexible body (ABEEM-7P), which couples the fluctuating partial charges calculated by atom-bond electronegativity equalization method (ABEEM). The ABEEM-7P model uses a slightly complicated tetrahedral geometry that is similar to that with the TIP5P model and introduces additional interaction sites, atoms, bonds, and lone-pair electrons, to describe the charge distribution in more detail, i.e., there are seven charged points (three atoms, two bonds, and two lone-pair electrons) in a monomer water, all of which are fluctuating with changing environments. Furthermore, the ABEEM/MM fluctuating charge model has been successfully applied to the water system [33, 34], ion–water system [35, 36], organic molecules [37], and peptides [38, 39]. Recently, the ABEEM/MM model has been used to perform dynamics simulations for proteins [40].

The primary aim of this work is to carry out a systemic study on the hydration of FA in terms of ab initio methods and the ABEEM$\sigma\pi$ fluctuating charge model. Meanwhile, the ABEEM$\sigma\pi$ was investigated extensively. The essence of the ABEEM$\sigma\pi$ model is to mimic the partial charges of all atoms, σ and π bonds, and lone-pair electrons in the electrostatic interaction term of the force field. In this paper, we put forward what, we believe, are now the most accurate results for the hydrogen bond interaction between the FA and water, as obtained from the high-level QM calculations. Then, we used the ABEEM$\sigma\pi$ fluctuating charge model to simulate the FA–$(H_2O)n$ ($n = 1$–3) clusters systemically. The reliability of these calculations has been confirmed in light of a comparison of geometrical and energetic properties with QM calculations. Furthermore, we have investigated the fine details of solvent effects on FA in aqueous solution by molecular dynamics simulation. The hydrogen-bonding pattern due to the interactions with water has been analyzed in detail. The remainder of this article is organized as follows. The methods and related details are summarized in Sect. 2. The results are discussed in Sect. 3. Finally, Sect. 4 gives the concluding remarks.

2 Computational methods

Based on fusing ABEEM$\sigma\pi$ model into molecular mechanics, the potential energy function, $E_{\mathrm{ABEEM}\sigma\pi/\mathrm{MM}}$, is shown in Eq. 1:

$$E_{\mathrm{ABEEM}\sigma\pi/\mathrm{MM}} = \sum_{\text{bonds}} k_{\mathrm{b}}(r - r_{\mathrm{eq}})^2 + \sum_{\text{angles}} k_{\theta}(\theta - \theta_{\mathrm{eq}})^2 + \sum_{\text{imptors}} v(1 - \cos 2\phi) + \sum_{\text{torsions}} \left\{ \frac{V_1}{2}[1 + \cos(\phi_i)] + \frac{V_2}{2}[1 - \cos(2\phi_i)] + \frac{V_3}{2}[1 + \cos(3\phi_i)] \right\} + \sum_{\text{nonbonded}} [kq_iq_je^2/r_{ij} + 4f_{ij}\varepsilon_{ij}(\sigma_{ij}^{12}/r_{ij}^{12} - \sigma_{ij}^{6}/r_{ij}^{6})] \quad (1)$$

It includes the bond stretching, angle bending, torsional rotation, and nonbonded interaction terms, i.e., a Coulomb term for the charge–charge interactions and a Lennard-Jones 12-6 term for the van der Waals repulsion and dispersion interaction. Here, k_{b}, k_{θ}, V_1, V_2, V_3 and v represent the force constants of bond stretching, angle bending, dihedral angle torsion, and improper torsion, respectively. r, θ and ϕ are actual values of bond lengths, bond angles, and dihedral angles. r_{eq} and θ_{eq} are used to denote the equilibrium values of the bond length and bond angle.

For van der Waals term, geometric combining rules for the Lennard-Jones coefficients are employed: $\sigma_{ij} = (\sigma_{ii}\sigma_{jj})^{1/2}$ and $\varepsilon_{ij} = (\varepsilon_{ii}\varepsilon_{jj})^{1/2}$. The summation runs over all pairs of atoms $i < j$ on molecules A and B or A and A for the intramolecular interactions. Moreover, in the latter case, the coefficient f_{ij} is equal to 0.0 for any i–j pair connected by a valence bond (1–2 pairs) or a valence bond angle (1–3 pairs). $f_{ij} = 0.5$ for 1,4 interactions (atoms separated by exactly three bonds) and $f_{ij} = 1.0$ for all of the other cases. For the Coulomb term, the partial charges q_i are obtained by atom-bond electronegativity equalization method (ABEEM$\sigma\pi$). The calculation detail of the charges in the ABEEM$\sigma\pi$ model is described in reference [39, 41, 42].

The electrostatic interaction energy E_{elec} is expressed by ABEEM$\sigma\pi$ model:

$$E_{\mathrm{elec}} = \sum_{i<j} kq_iq_j/r_{ij} \quad (2)$$

In Eq. 2, q_i and q_j are the partial charges of sites i and j, r_{ij} is separation of sites i and j, k is an overall correction coefficient 0.57 [43] in the ABEEM$\sigma\pi$ model if there is no otherwise specification. In this study, we use the ABEEM$\sigma\pi$ method to compute the partial charges of all atoms, bonds, lone-pair electrons and π bonds, then by Eq. 1 compute the total energy of the system, and when there is a change of bond, angle, dihedral angle or relative position of molecules, we recalculate the charges simultaneously, and then recalculate the total energy. In the hydrogen bond interaction region [33], k_{ij} is replaced by a $k_{\text{H-bond}}(R_{ij})$ function to describe the electrostatic interaction between the hydrogen atom and the lone-pair electron. In the present study, three types of $k_{\text{H-bond}}(R_{ij})$ functions are used for H-bonds C=O···Hw, H–O···Hw, and O–H···Ow, respectively. They are expressed as follows:

$$k(R_{\mathrm{lpOw-,H}}) = 0.605 - \frac{0.110}{1 + \exp[(R_{\mathrm{lpO=,H}} - 1.125)/0.147]} \quad (3)$$

$$k(R_{\mathrm{lpOw-,H}}) = 0.615 - \frac{0.102}{1 + \exp[(R_{\mathrm{lpOw-,H}} - 1.070)/0.133]} \quad (4)$$

$$k(R_{\mathrm{lpOw-,H}}) = 0.602 - \frac{0.112}{1 + \exp[(R_{\mathrm{lpOw-,H}} - 1.061)/0.140]} \quad (5)$$

Minimizations of isolated FA and FA–water clusters were performed with the limited memory BFGS quasi-newton nonlinear optimization routine. The criterion used for convergence was the root mean square (RMS) energy gradient less than 0.01 kcal/mol/Å. There was no any restraint, i.e., all atoms are allowed to move freely. Interaction energies were calculated for the FA–water hydrogen bond by taking the energy difference between the fragments and the complex.

$$E_{\mathrm{int}} = E_{(\mathrm{HCOOH})} + nE_{(\mathrm{H_2O})} - E_{(\mathrm{HCOOH}\cdots n\mathrm{H_2O})} \quad (6)$$

A classical molecular dynamics (MD) simulation was performed in terms of the ABEEM$\sigma\pi$/MM, starting with a (Z)-FA molecule in a cubic box of length 18.64 Å containing 212 H_2O molecules, large enough to contain the (Z)-FA and 0.8 nm of solvent on all sides. The system was optimized first, and then the MD simulation was carried out in the NVT ensemble, with periodic boundary condition and the minimum image convention. Temperature was kept constant at 298 K by Berendsen algorithm [44]. The equations of motion were solved using the velocity Verlet algorithm with a time step of 1 fs. The long-range interactions were truncated using a molecule-based cutoff

distance of 9.0 Å. The system was equilibrated within 300 ps, and the following 700 ps trajectory was collected for dynamical property analysis.

Quantum mechanical calculations were carried out for FA–(H_2O)n ($n = 1$–3) clusters. They were performed using the Gaussian 03 program package [45]. Geometries were optimized using the B3LYP method. For hydrogen bonding, it is expected that both diffuse and polarization functions may be necessary in the basis sets, thus the geometry optimization for complexes and their monomers was executed by using the basis sets aug-cc-pVTZ. Frequency calculations were also performed at this level of theory. Zero-point energies were computed using the harmonic vibrational frequencies at this level of theory. Zero-point energies taken from these frequency calculations can be assumed to be an upper limit due to the anharmonic nature of the potential energy surface [46]. Single-point energy calculations were conducted by using MP2 with aug-cc-pVTZ basis set. The basis set superposition error (BSSE) was evaluated by using the counterpoise correction method [47].

3 Results and discussion

In this section, we discuss the properties of the isolated FA, FA–water clusters and FA in aqueous solution by means of quantum mechanics (QM) methods and/or the ABEEM$\sigma\pi$/MM model. The calculated structures of FA and water using DFT method at aug-cc-pVTZ basis set and from ABEEM$\sigma\pi$/MM model are reported in Table 1. For comparison, results of DFT, MP2 at 6-311++g(2d,2p) level and the experimentally determined structures of FA and water, as well as the results from other force field are given in Table 1. We calculate two conformations of FA, denoted Z and E as shown in Fig. 1. Both conformations are planer. (Z)-FA has the acidic hydrogen aligned toward the oxygen atom of the carbonyl group, while (E)-FA has the hydrogen atom away from it. (Z)-FA is more stable than (E)-FA by about 3.90 ± 0.085 kcal/mol from microwave intensity measurements by Hocking [48]. The energy difference between the two configurations calculated by ABEEM$\sigma\pi$/MM model is 3.94 kcal/mol, AMBER is 4.82 kcal/mol [29], CHARMM is 5.97 kcal/mol [29], MMFF94 is

Table 1 Structural parameters for formic acid and water

Molecule	Coordinate	Exp[a]	DFT[b]	DFT[c]	MP2[d]	ABEEM$\sigma\pi$/MM	MM4[e]	MMFF94[f]
H_2O	O–H	0.957	0.964	0.961	0.958	0.9572		
	H–O–H	104.5	104.8	105.1	104.3	104.52		
Z-formic acid	C=O	1.202	1.198	1.198	1.205	1.203	1.2023	1.2165
	C–O	1.343	1.345	1.346	1.350	1.341	1.3489	1.3417
	C–H	1.097	1.096	1.096	1.091	1.101	1.0885	
	O–H	0.972	0.970	0.969	0.967	0.971	0.9671	0.9802
	O=C–O	124.9	125.1	125.1	125.0	124.9	124.0	121.8
	O–C–H	111	109.7	109.7	109.8	111.1	110.5	
	C–O–H	106.3	107.8	107.7	106.8	106.4	106.6	104.3
	H–C=O	124.8	125.1	125.2	125.2	124.1		
E-formic acid	C=O	1.195	1.191	1.191	1.198	1.197	1.1955	1.2172
	C–O	1.352	1.352	1.353	1.357	1.349	1.3490	1.3417
	C–H	1.105	1.102	1.102	1.097	1.101	1.0955	
	O–H	0.956	0.965	0.964	0.962	0.960	0.9614	0.9761
	O=C–O	122.1	122.4	122.6	122.5	121.8	122.0	124.3
	O–C–H	114.6	113.5	113.6	113.5	114.4	112.3	
	C–O–H	109.7	110.2	110	108.9	109.3	109.4	112
	H–C=O		124.0	123.9	124.0	123.8		

All bond lengths are reported in angstroms, all angles are in deg

[a] Reference [50]: (Z)-formic geometries, and Ref. [49]: (E)-formic geometries

[b] Geometry optimization at the B3LYP/aug-cc-pVTZ level in this work

[c] Geometry optimization at the B3LYP/6-311++G(2d,2p) level from Ref. [12]

[d] Geometry optimization at the MP2/6-311++G(2d,2p) level from Ref. [25]

[e] Reference [25]

[f] Reference [27]

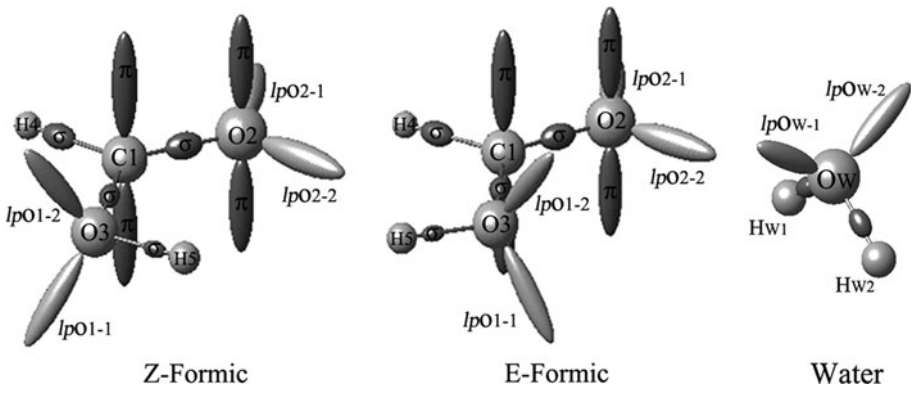

Fig. 1 The configurations of Z (E)-Formic acid and water. The atoms, σ and π bonds, and lone-pair electrons sites are shown

4.89 kcal/mol [27], and MM3 is 3.98 kcal/mol [26]. Compared with other force fields, the calculated result from the ABEEM$\sigma\pi$/MM model is in good agreement with the experimental value.

Seen from Table 1, comparison of the structures for the isolated FA and water shows good agreement for the bond lengths, bond angles between ABEEM$\sigma\pi$/MM model and the experimental data [49, 50]. All experimental, QM and ABEEM$\sigma\pi$/MM results show that the C=O bond is longer in the Z-form than in the E-form (1.202 Å vs. 1.195 Å, respectively), but the trend in the C–O bond length is reversed (1.343 Å vs. 1.352 Å, respectively). These phenomena can be explained by the fact that the lone pairs on the carboxylic oxygen are better positioned for O=C–O resonance in the Z-form, but seen from the Table 1 the other force fields [25, 27] do not show these phenomena. Considering all geometric parameters obtained with different theoretical models and basis sets, the difference between the B3LYP/aug-cc-pVTZ calculated and experimental results may be negligible. The calculated harmonic vibrational frequencies for both conformations of FA by DFT and ABEEM$\sigma\pi$/MM model versus the experimental frequencies [51] are shown in Fig. 2. Obviously, the agreement between them is satisfactory.

The ABEEM$\sigma\pi$/MM model makes a full consideration on the conformational changes and gives the explicitly quantitative charges of all molecular regions, such as atoms, σ and π bonds, and lone-pair electrons. The charges of the isolated FA, H_2O and FA–water complexes calculated by the ABEEM$\sigma\pi$/MM model are listed in Table 2 (see Fig. 1, the structure and numbering of isolated FA and water). The charge distributions of isolated (Z)-FA and (E)-FA are very different from each other, which is mainly due to the intramolecular environment changes. This is the merit of our ABEEM$\sigma\pi$ fluctuating force field, i.e., charges fluctuating upon the ambient environment. In addition, the dipole moments of the two conformers are 1.413 and 3.779 D for the ABEEM$\sigma\pi$/MM model, respectively, and are presented in Table 3 as well as the comparison with experimental data and other force field results. The dipole

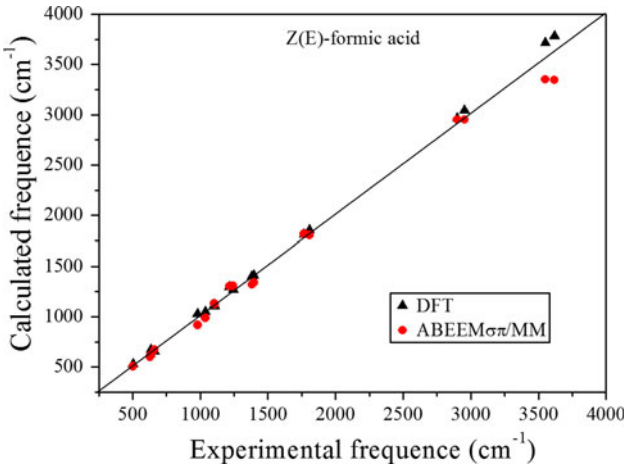

Fig. 2 The vibrational frequencies calculated by DFT and ABEEM$\sigma\pi$/MM model versus the experimental frequencies for Z (E)-Formic acid

moment of water in gas phase also listed in Table 3. Seen from Table 3, the (E)-FA has a higher dipole moment than the (Z)-FA, and the ABEEM$\sigma\pi$/MM model and the DFT method at aug-cc-pVTZ level give relatively good agreement with the experimental values.

3.1 Properties of FA and water clusters

3.1.1 FA and one water complexes

Six configurations of the complex between FA and one water molecule have been studied here. Three of these are with (Z)-FA and three are with (E)-FA and all structures are shown in Fig. 3. No imaginary vibrations were calculated in the frequency analysis of these structures. The structural parameters from ABEEM$\sigma\pi$/MM model and B3LYP/aug-cc-pVTZ level calculation are listed in Table 4. The optimized geometries of the FA complexes with one water from ABEEM$\sigma\pi$/MM model are in good agreement with the high-level QM method calculations.

The most stable conformation is a cycle complex (FAZ1) with both the water and the FA acting as hydrogen

Table 2 Charge distributions of isolated formic acid, H_2O, and formic acid–H_2O complexes by the ABEEM$\sigma\pi$/MM model

	Isomer		FAZ1	FAZ2	FAZ3	FAE1	FAE2	FAE3
	Z-formic	E-formic						
C1	0.5015	0.5001	0.5012	0.5099	0.5150	0.4946	0.5084	0.5124
O2	0.0197	0.0207	0.0223	**0.0224**	0.0199	0.0204	**0.0234**	**0.0251**
O3	0.0097	0.0087	0.0090	0.0097	**0.0147**	0.0082	0.0087	0.0087
H4	0.1777	0.1613	0.1788	0.1884	0.1921	0.1597	0.1729	0.1695
H5	0.2896	0.2676	**0.3362**	0.2947	0.2956	**0.3094**	0.2751	0.2768
OW	0.0948	0.0948	0.1012	0.0974	0.0975	0.0998	0.0977	0.0977
HW1	0.2887	0.2887	0.2776	0.2624	**0.3429**	**0.3165**	**0.3562**	0.2437
HW2	0.2887	0.2887	**0.3760**	**0.3546**	0.2697	**0.3162**	0.2642	**0.3737**
σC1–H4	−0.1177	−0.1179	−0.1179	−0.1181	−0.1183	−0.1176	−0.1184	−0.1184
σC1–O2	−0.1252	−0.1240	−0.1249	−0.1251	−0.1256	−0.1242	−0.1240	−0.1238
σC1–O3	−0.0986	−0.0982	−0.0986	−0.0986	−0.0982	−0.0983	−0.0982	−0.0983
σO3–H5	−0.0781	−0.0779	−0.0813	−0.0783	−0.0781	−0.0810	−0.0783	−0.0783
σOw–Hw1	−0.1461	−0.1461	−0.1495	−0.1491	−0.1477	−0.1463	−0.1464	−0.1504
σOw–Hw2	−0.1461	−0.1461	−0.1467	−0.1463	−0.1487	−0.1463	−0.1491	−0.1459
lpO2-1	−0.1448	−0.1262	**−0.1968**	−0.1408	−0.1408	−0.1337	−0.1221	**−0.1704**
lpO2-2	−0.1406	−0.1403	−0.1412	**−0.1849**	−0.1352	−0.1481	**−0.1848**	−0.1433
lpO1-1	−0.1199	−0.1111	−0.1149	−0.1138	**−0.1445**	−0.1178	−0.1064	−0.1058
lpO1-2	−0.1199	−0.1111	−0.1185	−0.1138	**−0.1449**	−0.1178	−0.1063	−0.1059
lpOw-1	−0.1900	−0.1900	**−0.2547**	−0.2095	−0.2049	−0.1995	−0.2122	−0.2094
lpOw-2	−0.1900	−0.1900	−0.2039	−0.2096	−0.2088	**−0.2404**	−0.2105	−0.2094
πC1-1	−0.0140	−0.0140	−0.0138	−0.0138	−0.0137	−0.0142	−0.0138	−0.0138
πC1-2	−0.0140	−0.0140	−0.0140	−0.0138	−0.0138	−0.0142	−0.0139	−0.0138
πO2-1	−0.0128	−0.0119	−0.0124	−0.0121	−0.0122	−0.0127	−0.0112	−0.0105
πO2-2	−0.0128	−0.0119	−0.0131	−0.0121	−0.0122	−0.0127	−0.0113	−0.0104

All calculated charges in au

The remarkable changes of charges were shown in bold

Table 3 Dipole moments (D) of the gas phase for (Z),(E)-formic acid and water

Isomer	Exp	DFT[d]	DFT[e]	MP2[f]	MM4[g]	MM3[h]	ABEEM$\sigma\pi$/MM
(Z)-formic acid	1.42[a]	1.544	1.531	1.735	1.443	1.730	1.413
(E)-formic acid	3.79[b]	3.915	3.972	4.405	3.769	3.890	3.779
H_2O	1.855[c]	1.847	1.959	2.065			1.857

[a] Reference [54]

[b] Reference [48]

[c] Reference [55]

[d] The QM results at B3LYP/aug-cc-pVTZ level

[e] The QM results at B3LYP/6-311++G(2d,2p) level

[f] The QM results at MP2/6-311++G(2d,2p) level from Ref. [25]

[g] Reference [25]

[h] Reference [26]

[g] The results calculated by Molecular Mechanics (MM4) from Ref. [25]

[h] The results calculated by Molecular Mechanics (MM3) from Ref. [26]

donor and acceptor, respectively, resulting in two relatively strong hydrogen bonds. Among the six complexes of FA with one water, this is the only one that has been observed experimentally [8, 10]. The study by Priem et al. [10] observed this complex using microwave spectroscopy. They also performed ab initio calculations at the MP2/6-311++g(3df,2p) level of theory. We designate hydrogen bonds in which the FA is acting as a hydrogen donor to the

water as R1 (H-bond O–H···Ow) and hydrogen bonds in which the water is donating a hydrogen atom to the carbonyl oxygen atom as R2 (H-bond C=O···Hw). For FAZ1, The R1 and R2 are 1.795 and 2.095 Å, respectively, from ABEEM$\sigma\pi$/MM model and 1.786 and 2.019 Å, respectively, from B3LYP/aug-cc-pVTZ level calculation. Consistent with the structure determined by observed moments of inertia by Priem et al. [10] (1.810 and 2.210 Å) and in agreement with the calculations presented both in that work (1.779 and 2.025 Å) and in the work by Rablen et al. [11] (1.775 and 2.016 Å). Moreover, our calculations agree with those in the work [7, 12] calculated at high QM method. In FAZ2 and FAZ3, there is one hydrogen bond of the type R2 and R3, respectively. As one might expect, this interaction, R3 (H-bond H–O···Hw), is not strong, which is 2.234 from ABEEM$\sigma\pi$/MM and 2.217 from B3LYP/aug-cc-pVTZ level calculation. There are other three structures of complexes with (E)-FA: FAE1, FAE2, FAE3. And all of these structures have one hydrogen bond of type R1, R2 and R2, respectively. Among all of the intermolecular H-bonds for these six complexes, the average H-bond lengths (shown in Table 5) of O–H···Ow, C=O···Hw and H–O···Hw in FA–H_2O complexes are 1.840, 2.041 and 2.234 Å from ABEEM$\sigma\pi$/MM, which are close to the corresponding DFT values (1.801, 2.009 and 2.217 Å, respectively).

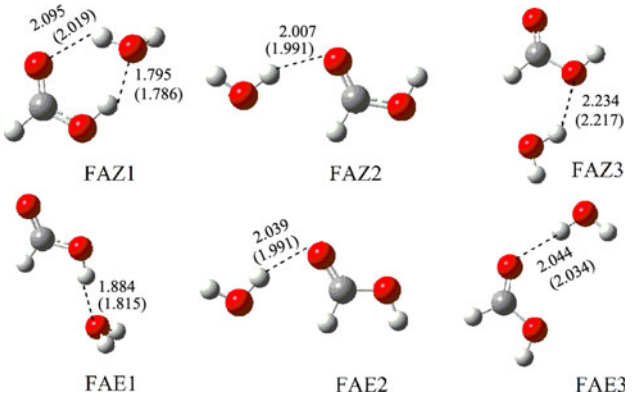

Fig. 3 Formic acid complexes with one water molecules. *Dashed lines* indicate hydrogen bonding

The charges of FA–water systems with one water molecule are listed in Table 2. When compared with isolated formic and water molecules, the charges are different for all sites, which is consequential upon environment changes, i.e., the different position of water molecule relative to FA affects the redistribution of the electron cloud. The remarkable change of charges takes place at the position where the hydrogen bond forms. For example, obvious polarization takes place for the charges of H5, lpOw-1, Hw2, and lpO2-1 in FAZ1 (see Fig. 3 for the notation of charge sites of FA and H_2O molecules), i.e., qH5 and qHw2 are 0.3362 and 0.3760 versus 0.2896 and 0.2897 in isolated molecules, and the charges of lpO2-1 (−0.1968) and lpOw-1 (−0.2547) are more negative than those of −0.1448 and −0.1908 in isolated FA and H_2O molecules. In the same way, this obvious polarization also takes place for other clusters. To summarize, the fluctuating charges of the FA and the water molecules can correctly reflect the redistribution with the changed ambient environment and make a compensation for the shortages of fixed-point charge models. Meanwhile, the fluctuating charges are very important in the calculations of the interaction energies.

Table 6 lists the interaction energies of FA–H_2O complexes from ABEEM$\sigma\pi$/MM model and several ab initio calculations [7, 12]. All of the QM studies about the FA complexes with one water molecule show that the energy and the relative stability order of these conformations is FAZ1 > FAE1 > FAE2 > FAZ2 > FAE3 > FAZ3. The interaction energies of the FA–H_2O complexes from the

Table 4 Formic acid bond distance (Å) of HCOOH–(H_2O) complexes from ABEEM$\sigma\pi$/MM model and B3LYP/aug-cc-pVTZ level calculations

Dimer	Geometry	C=O	O–H	H–C	C–O	R(1)	R(2)	R(3)
FAZ1	ABEEM$\sigma\pi$/MM	1.207	0.970	1.099	1.341	1.795	2.095	
	B3LYP	1.210	0.990	1.096	1.326	1.786	2.019	
FAZ2	ABEEM$\sigma\pi$/MM	1.203	0.972	1.101	1.338		2.007	
	B3LYP	1.204	0.971	1.094	1.337		1.991	
FAZ3	ABEEM$\sigma\pi$/MM	1.202	0.971	1.100	1.340			2.234
	B3LYP	1.196	0.97	1.094	1.355			2.217
FAE1	ABEEM$\sigma\pi$/MM	1.198	0.972	1.103	1.346	1.884		
	B3LYP	1.196	0.978	1.103	1.34	1.815		
FAE2	ABEEM$\sigma\pi$/MM	1.198	0.961	1.105	1.345		2.039	
	B3LYP	1.197	0.965	1.1	1.344		1.991	
FAE3	ABEEM$\sigma\pi$/MM	1.197	0.960	1.100	1.350		2.044	
	B3LYP	1.194	0.966	1.1	1.346		2.034	

Table 5 Average H-bond length (Å) for FA–$(H_2O)n$ ($n = 1$–3) cluster from ABEEM$\sigma\pi$/MM model and B3LYP/aug-cc-pVTZ level calculations

	FA–H_2O		FA–$(H_2O)_2$		FA–$(H_2O)_3$	
	ABEEM$\sigma\pi$/MM	B3LYP	ABEEM$\sigma\pi$/MM	B3LYP	ABEEM$\sigma\pi$/MM	B3LYP
O–H···Ow	1.840	1.801	1.799	1.721	1.774	1.692
C=O···Hw	2.041	2.009	1.988	1.965	1.976	1.928
H–O···Hw	2.234	2.217	2.192	2.181	2.064	2.038

Table 6 Interaction energies (in kcal/mol) of HCOOH–H_2O complexes

Complex	ABEEM$\sigma\pi$/MM	Ab initio			Deviation[d]
		MP2[a]	B3LYP[b]	B3LYP[c]	
FAZ 1	6.79	7.14	7.0	9.1	−0.35
FAZ 2	2.94	3.33	3.0	4.3	−0.39
FAZ 3	1.91	2.10	1.3	2.4	−0.19
FAE 1	5.21	6.13	6.9	7.5	−0.92
FAE 2	4.18	3.75	3.4	4.8	0.44
FAE 3	3.15	2.53	2.5	3.8	0.62

[a] Energies obtained at MP2/aug-cc-pVTZ//B3LYP/aug-cc-pVTZ level with BSSE and ZPE corrections. Zero-point-energy calculated at B3LYP/aug-cc-pVTZ level in this work

[b] Reference [7]: at the B3LYP/6-311++G(2d,2p)//B3LYP/6-311++G(d,p) lever with BSSE and ZPE corrections

[c] Reference [12]: at the B3LYP/6-311++G(2d,2p)//B3LYP/6-311++G(2d,2p) lever with BSSE corrections

[d] The deviation of interaction energies between ABEEM$\sigma\pi$/MM and MP2/aug-cc-pVTZ//B3LYP/aug-cc-pVTZ level

ABEEM$\sigma\pi$/MM model are in agreement with the QM calculations at the MP2/aug-cc-pVTZ//B3LYP/aug-cc-pVTZ level. The most stable conformation is FAZ1 having one hydrogen bond of the first type and one hydrogen bond of the second type, and FAZ3 has the lowest interaction energy due to the relative weak H-bond between water hydrogen atom and the oxygen (HO) bound to the acidic hydrogen on the FA. The energy order from ABEEM$\sigma\pi$/MM model agrees with the QM results, and the deviations are within 1.0 kcal/mol.

3.1.2 FA and two water complexes

Previously, (Z)-FA is about 1,000 times more abundant than (E)-FA at room temperature [52]. We will focus on the *Z* configuration of FA when calculating structures with more than one water molecule [7]. We have studied six complexes of FA with two water molecules. All of these have FA in the *Z* configuration and are shown in Fig. 4. The structural parameters from ABEEM$\sigma\pi$/MM model and B3LYP/aug-cc-pVTZ level calculation are listed in Table 7. As seen from the Table 7, the optimized geometries of the FA complexes with two water molecules from

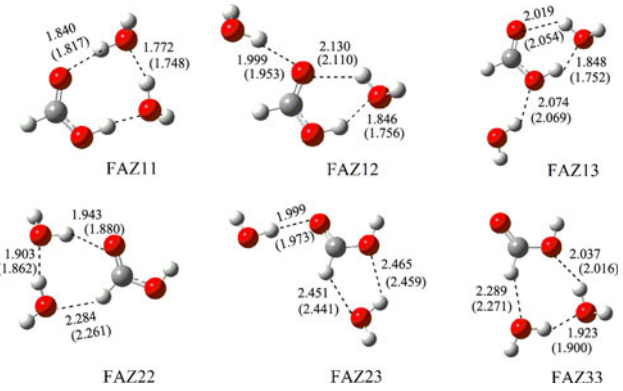

Fig. 4 Formic acid complexes with two water molecules. *Dashed lines* indicate hydrogen bonding

the ABEEM$\sigma\pi$/MM model is in agreement with those from the B3LYP/aug-cc-pVTZ level.

FAZ11 has been observed in laboratory experiments using microwave spectroscopy [10]. To the best of our knowledge, the others structures have not been investigated using microwave spectroscopy. FAZ11 is the most stable configure of these complexes, which forms an eight-member ring with both the water and the FA acting as hydrogen donor and acceptor, resulting in two relatively strong hydrogen bonds, and the R1 is 1.703 Å, and the R2 is 1.840 Å, from the ABEEM$\sigma\pi$/MM model, which is in good agreement with the calculated results from the B3LYP/aug-cc-pVTZ level (1.654 and 1.817 Å, respectively), and other reported ab initio calculations, such as in the work by Aloisio et al. [7] (1.662 and 1.841 Å) and in the work by Zhou et al. [12] (1.663 and 1.843 Å). Besides, the two water molecules also form a hydrogen bond, and the bond length (1.772 Å) by the ABEEM$\sigma\pi$/MM model is slightly longer than that of 1.748 Å from B3LYP/aug-cc-pVTZ level calculations. To summarize, the average H-bond lengths (shown in Table 5) of O–H···Ow, C=O···Hw and H–O···Hw in FA–$(H_2O)_2$ complexes are 1.799, 1.988, and 2.192 Å from ABEEM$\sigma\pi$/MM, which are close to the corresponding DFT values (1.721, 1.965, and 2.181 Å, respectively). In addition, the bond length of C=O and C–O is elongated to some extent due to the formation of two hydrogen bonds.

Table 7 Formic acid bond distance (Å) of HCOOH–$(H_2O)_2$ complexes from ABEEM$\sigma\pi$/MM model and B3LYP/aug-cc-pVTZ level calculations

Dimer	Geometry	C=O	O–H	H–C	C–O	R(1)	R(2)	R(2)′	R(3)	R(4)	R(W)
FAZ 11	ABEEM$\sigma\pi$/MM	1.193	0.963	1.096	1.319	1.703	1.840				1.772
	B3LYP	1.214	1.005	1.096	1.314	1.654	1.817				1.748
FAZ 12	ABEEM$\sigma\pi$/MM	1.207	0.970	1.101	1.319	1.846	2.130	1.999			
	B3LYP	1.216	0.992	1.094	1.319	1.756	2.110	1.953			
FAZ 13	ABEEM$\sigma\pi$/MM	1.205	0.968	1.100	1.341	1.848	2.019		2.074		
	B3LYP	1.208	0.992	1.095	1.334	1.752	2.054		2.069		
FAZ 22	ABEEM$\sigma\pi$/MM	1.205	0.972	1.101	1.337		1.943			2.284	1.903
	B3LYP	1.209	0.971	1.095	1.336		1.880			2.261	1.862
FAZ 23	ABEEM$\sigma\pi$/MM	1.202	0.972	1.103	1.340		1.999		2.465	2.451	
	B3LYP	1.203	0.971	1.093	1.345		1.973		2.459	2.441	
FAZ 33	ABEEM$\sigma\pi$/MM	1.200	0.971	1.100	1.351				2.037	2.289	1.923
	B3LYP	1.196	0.97	1.095	1.364				2.016	2.271	1.900

Table 8 Interaction energies (in kcal/mol) of HCOOH–$(H_2O)_2$ complexes

Complex	ABEEM$\sigma\pi$/MM	Ab initio			Deviation[d]
		MP2[a]	B3LYP[b]	B3LYP[c]	
FAZ 11	16.19	15.96	19.8	21.8	0.23
FAZ 12	10.17	10.38	14.0	14.3	−0.21
FAZ 13	8.46	9.34	12.7	12.6	−0.88
FAZ 22	10.10	9.70	13.0	13.3	0.41
FAZ 23	6.26	4.94	8.1	6.3	1.32
FAZ 33	8.26	7.40	10.3	10.1	0.86

[a] Energies obtained at MP2/aug-cc-pVTZ//B3LYP/aug-cc-pVTZ level with BSSE and ZPE corrections. Zero-point-energy calculated at B3LYP/aug-cc-pVTZ level in this work

[b] Reference [7]: at the B3LYP/6-311++G(2d,2p)//B3LYP/6-311++G(d,p) lever with BSSE and ZPE corrections

[c] Reference [12]: at the B3LYP/6-311++G(2d,2p)//B3LYP/6-311++G(2d,2p) lever with BSSE corrections

[d] The deviation of interaction energies between ABEEM$\sigma\pi$/MM and MP2/aug-cc-pVTZ//B3LYP/aug-cc-pVTZ level

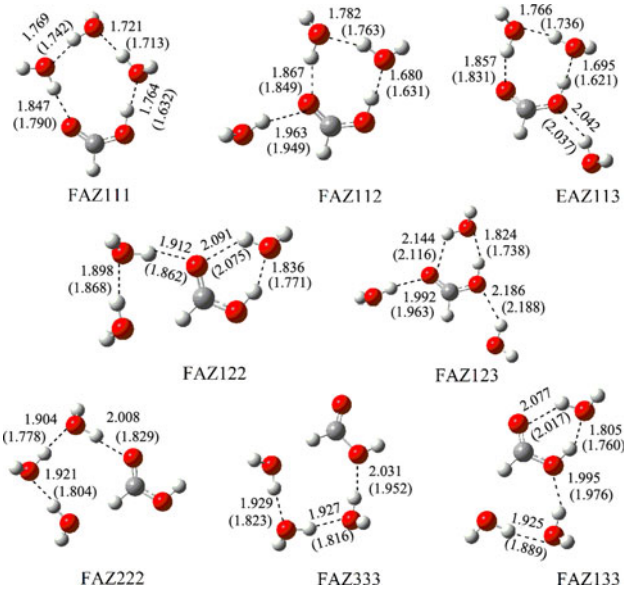

Fig. 5 Formic acid complexes with three water molecules. *Dashed lines* indicate hydrogen bonding

From the interaction energies of FA–$(H_2O)_2$ complexes reported in Table 8, we can found that FAZ11 has the highest energy compared with the other conformations, and the relative stability order of these conformations is FAZ11 > FAZ12 > FAZ22 > FAZ13 > FAZ33 > FAZ23 from the ABEEM$\sigma\pi$/MM model and the MP2/aug-cc-pVTZ//B3LYP/aug-cc-pVTZ level calculations.

3.1.3 FA and three water complexes

In the present study, eight configurations are taken into consideration when three water molecules are bound to FA. The graphical representations of the FA–$(H_2O)_3$ clusters are shown in Fig. 5. The geometric parameters for these structures are given in Table 9. Three of the structures FAZ111, FAZ222, and FAZ333 are ring-like structures similar to water tetramer. Another four structures FAZ112, FAZ113, FAZ122, and FAZ133 are ring-like species similar to water trimer. The FAZ123 structure has a water molecule on each of the three bonding sites on the FA molecule.

As seen from the Table 9, the optimized geometries of the FA complexes with three water molecules from the ABEEM$\sigma\pi$/MM model are close to those from the B3LYP/aug-cc-pVTZ level. It is denoted that both the ABEEM$\sigma\pi$/MM model and B3LYP/aug-cc-pVTZ calculated structures tend to have longer C=O and O–H, but a shorter C–O bond lengths. FAZ123 structure has one water molecule at each

Table 9 Formic acid bond distance (Å) of HCOOH–$(H_2O)_3$ complexes from ABEEM$\sigma\pi$/MM model and B3LYP/aug-cc-pVTZ level calculations

Dimer	Geometry	C=O	O–H	H–C	C–O	R(1)	R(2)	R(2)′	R(3)	R(W)
FAZ 111	ABEEM$\sigma\pi$/MM	1.205	0.977	1.091	1.325	1.764	1.847			1.769
										1.721
	B3LYP	1.214	1.007	1.097	1.311	1.632	1.79			1.742
										1.713
FAZ 112	ABEEM$\sigma\pi$/MM	1.209	1.004	1.098	1.309	1.680	1.867	1.963		1.782
	B3LYP	1.221	1.008	1.095	1.306	1.631	1.849	1.949		1.763
FAZ 113	ABEEM$\sigma\pi$/MM	1.194	1.060	1.098	1.328	1.695	1.857		2.042	1.766
	B3LYP	1.211	1.01	1.096	1.321	1.621	1.831		2.037	1.736
FAZ 122	ABEEM$\sigma\pi$/MM	1.215	1.019	1.098	1.329	1.836	2.091	1.912		1.898
	B3LYP	1.222	0.991	1.094	1.318	1.771	2.075	1.862		1.868
FAZ 123	ABEEM$\sigma\pi$/MM	1.206	0.998	1.102	1.329	1.824	2.144	1.992	2.186	
	B3LYP	1.214	0.994	1.093	1.326	1.738	2.116	1.963	2.188	
FAZ 133	ABEEM$\sigma\pi$/MM	1.206	0.989	1.096	1.336	1.805	2.077		1.995	1.925
	B3LYP	1.208	0.992	1.095	1.340	1.76	2.017		1.976	1.889
FAZ 222	ABEEM$\sigma\pi$/MM	1.205	0.969	1.095	1.336			2.008		1.904
										1.921
	B3LYP	1.211	0.971	1.096	1.336			1.829		1.778
										1.804
FAZ 333	ABEEM$\sigma\pi$/MM	1.203	0.969	1.096	1.343				2.031	1.927
										1.929
	B3LYP	1.196	0.97	1.096	1.367				1.952	1.816
										1.823

Table 10 Interaction energies (in kcal/mol) of HCOOH–$(H_2O)_3$ complexes

Complex	ABEEM$\sigma\pi$/MM	Ab initio			Deviation[d]
		MP2[a]	B3LYP[b]	MP2[c]	
FAZ 111	23.32	21.84	26.3	31.1	1.48
FAZ 112	19.64	18.71	22.7	27.3	0.93
FAZ 113	17.10	18.22	21.6	26.3	−1.12
FAZ 122	17.03	16.72	19.8	25.1	0.31
FAZ 123	11.44	12.39	15.4	19.3	−0.95
FAZ 133	14.75	15.00	17.8	23.2	−0.25
FAZ 222	16.70	16.34	19.4	24.2	0.36
FAZ 333	15.97	16.21	16.2	21.1	−0.24

[a] Energies obtained at MP2/aug-cc-pVTZ//B3LYP/aug-cc-pVTZ level with BSSE and ZPE corrections. Zero-point-energy calculated at B3LYP/aug-cc-pVTZ level in this work

[b] Reference [7]: at the B3LYP/6-311++G(2d,2p)//B3LYP/6-311++G(d,p) lever with BSSE and ZPE corrections

[c] Reference [7]: at the MP2/6-311++G(2d,2p)//B3LYP/6-311++G(d,p) lever with BSSE corrections

[d] The deviation of interaction energies between ABEEM$\sigma\pi$/MM and MP2/aug-cc-pVTZ//B3LYP/aug-cc-pVTZ level

bonding site, similar to the three complexes of (Z)-FA with one water molecule. Every intermolecular bond in FAZ123 is shorter than the bond in FAZ1, FAZ2, and FAZ3, and the geometry of the FA molecule is altered compared with the isolate FA.

Their interaction energy values are shown in Table 10, as well as the comparison with those from the MP2/aug-cc-pVTZ//B3LYP/aug-cc-pVTZ level QM calculations. The interaction energy values of FA–$(H_2O)_3$ by the ABEEM$\sigma\pi$/MM model are found to be in good agreement with those from ab initio calculations, within the deviation of 1.50 kcal/mol. The interaction energy order of these conformations is FAZ111 > FAZ112 > FAZ113 > FAZ122 > FAZ222 > FAZ333 > FAZ133 > FAZ123 from the ABEEM$\sigma\pi$/MM model and the MP2/aug-cc-pVTZ//B3LYP/aug-cc-pVTZ level calculations.

For a clear comparison, the interaction energies of FA–$(H_2O)n$ (n = 1–3) clusters from both the ABEEM$\sigma\pi$/MM model and ab initio methods are displayed in Fig. 6, where the linear correlation analysis is shown in the inner panel. The linear coefficient reaches 0.993, and the root mean square deviation (RMSD) is 0.74 kcal/mol. These results show that the ABEEM$\sigma\pi$/MM model can give the overall interaction energy properties in good agreement with the high-level QM calculations on FA–water complexes.

In addition, the optimization of (Z)-FA in aqueous solution has been done by ABEEM$\sigma\pi$/MM and the explicit ABEEM-7P water solvent model. For comparison, the

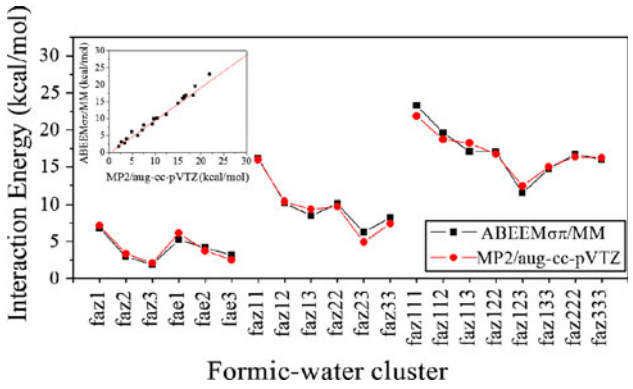

Fig. 6 Scatter plots comparing the MP2/aug-cc-pVTZ//B3LYP/aug-cc-pVTZ and ABEEM$\sigma\pi$/MM interaction energies of Formic acid–$(H_2O)n$ (n = 1–3) complexes

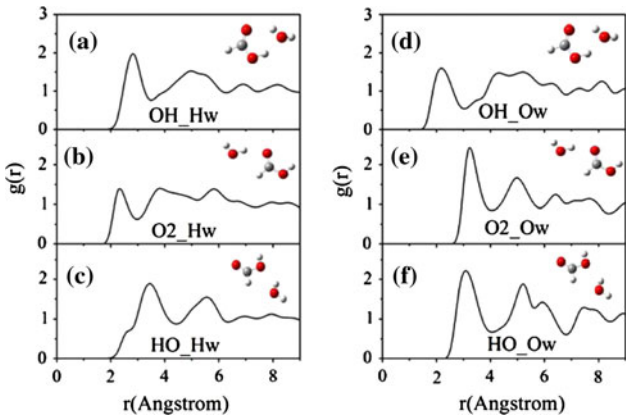

Fig. 7 Radial distribution functions for water hydrogen atoms (Hw) around the acidic hydrogen (OH) on the formic acid (**a**), the oxygen atom (O2) of the carbonyl group (**b**) and the oxygen (HO) bound to the acidic hydrogen on the formic acid (**c**). Radial distribution functions for water oxygen atoms (Ow) around the acidic hydrogen (OH) on the formic acid (**d**), the oxygen atom (O2) of the carbonyl group (**e**) and the oxygen (HO) bound to the acidic hydrogen on the formic acid (**f**)

optimization of (Z)-FA in aqueous solution has been done with B3LYP/aug-cc-PVTZ, the solution effects has been modeled with the SCIPCM [53] (self-consistent isodensity continuum model) method. The calculated structures of FA by ABEEM$\sigma\pi$/MM and DFT method are listed in Table 11. Seen from the Table 11, the optimized geometries of (Z)-FA by ABEEM$\sigma\pi$/MM and ABEEM-7P water solvent model are close to those from the B3LYP/aug-cc-pVTZ level with the SCIPCM method. Only the C–O length and the angle C–O–H increase to some extent relative to those from the SCIPCM method and this can be explained by the strong H-bond polarization effect between the acidic hydrogen (OH) on the FA with water oxygen.

3.2 Radial distribution

Next, the dynamic simulation of (Z)-FA in aqueous solution based on the ABEEM$\sigma\pi$/MM have been performed in the present work. Radial distribution function (RDF) is a useful tool to describe the structure of a system, particularly of liquids, and the peaks of the RDF can reflect the shell structure of the solvent. Here, the structure feature of the water molecules surrounding the FA is described by the RDFs of the Hw atoms of H_2O molecules around the acidic hydrogen (OH) on the FA (Fig. 7a), the oxygen atom (O2) of the carbonyl group (Fig. 7b) and the oxygen (HO) bound to the acidic hydrogen on the FA (Fig. 7c). The RDFs of the Ow atoms of H_2O molecules around the FA molecule are presented in (Fig. 7d–f, respectively). The OH–Ow RDF (solid line) shows a well-defined and more pronounced first peak located at 2.1 Å corresponding to the first hydration shell, followed by a broader second peak centered at about 5.0 Å and the third peak is very weak at about 6.5 Å. On the other hand, OH–Hw RDF (solid line) is a sharp peak located at about 2.9 Å, followed by a lower and broader second peak centered at about 5.2 Å and the third peak is weak. The OH–Ow and OH–Hw RDF have well-defined first peaks, indicating strong hydrogen-bonding interaction between the acidic hydrogen (OH) on the FA with water oxygen. It also implies that the FA can influence about two solvation shells from the ABEEM$\sigma\pi$/MM MD simulation.

The RDFs of water molecules with respect to the oxygen atom (O2) of the carbonyl group are shown in Fig. 7b and f. The O2-Hw and O2-Ow distributions have well-defined first peaks, at 2.3 and 3.3 Å, respectively, indicating strong hydrogen-bonding interactions between the carbonyl

Table 11 Structural parameters for (Z)-formic acid in aqueous solution

(Z)-formic acid	Bond length (Å)				Bond angle (°)			
	C=O	C–O	C–H	O–H	O=C–O	O–C–H	C–O–H	H–C=O
ABEEM$\sigma\pi$/MM (TIP-7P)[a]	1.173	1.356	1.112	0.972	125.0	109.5	103.3	125.6
DFT (SCIPCM)[b]	1.204	1.336	1.095	0.971	125.2	110.2	109.5	124.7

[a] Geometry optimization in the explicit ABEEM-7P water solvent model

[b] Geometry optimization at the B3LYP/aug-cc-pVTZ level. For the solvent calculations by the SCIPCM (self-consistent isodensity continuum model) method [53]

oxygen with water hydrogen. A second peak can be distinguished at 3.8 and 5.1 Å, respectively, and the third peaks are weak. For the RDFs of water molecules with respect to oxygen (HO) bound to the acidic hydrogen on the FA are shown in Fig. 7c and f. The first peak in HO–Ow RDF located at 3.1 Å and the HO–Hw RDF appears not very structured, which means that the first solvation shell likely has a fluctuational character and a not very strong hydrogen-bonding interactions between oxygen (HO) bound to the acidic hydrogen with water hydrogen, and this is consistent with the conclusion that is obtained from the study on complexes of FA and water.

4 Conclusion

We have systemically studied the hydrogen bond interaction of complexes between FA and water (with up to three water molecules) by ab initio methods and the ABEEM$\sigma\pi$ fluctuating charge force filed. The B3LYP/aug-cc-pVTZ predicts the geometries in good agreement with the experimental values for isolate FA molecules and the FA–water compounds than those found with other theoretical levels. The ABEEM$\sigma\pi$/MM model gives reasonable energies and geometries of these clusters by taking the ABEEM$\sigma\pi$ charges of all atoms, σ and π bonds, and lone-pairs into the electrostatic interaction term. For the interaction energies, the linear coefficient reaches 0.993, and the RMSD is 0.74 kcal/mol when compared with the present ab initio calculations at the MP2/aug-cc-pVTZ//B3LYP/aug-cc-pVTZ level. Molecular dynamic simulation of FA in aqueous solution has been carried out by ABEEM$\sigma\pi$/MM model. Through analysis of the RDF of water molecule around the FA, it is drawn that there are three hydrogen bonds patterns, and strong hydrogen-bonding interaction between the acidic hydrogen on the FA and the carbonyl oxygen with water hydrogen. There is a not very strong hydrogen-bonding interaction between oxygen bound to the acidic hydrogen with water hydrogen.

In conclusion, the ABEEM$\sigma\pi$ fluctuating charge force field can reasonably reflect interaction between FA and water, and this model may be developed to study the hydration of other organic acids.

5 Supporting information available

The parameters of the ABEEM/MM fluctuating charge model for formic acid are included in the "Electronic Supplementary Material".

Acknowledgments We are very grateful to the editor and reviewers' nice suggestions on the manuscript. We also greatly thank Professor Jay William Ponder for providing the Tinker programs. This work was supported by the grant from the National Natural Science Foundation of China (No. 20633050, 20703022 and 20873055).

References

1. Graedel TE, Weschler CJ (1981) Rev Geophys Space Phys 19:505–539
2. Zhao J, Khalizov A, Zhang R (2009) J Phys Chem A 113:680–689
3. Aloisio S, Francisco JS (2000) J Am Chem Soc 122:9196–9200
4. Henon E, Canneaux S, Bohr F, Dóbé S (2003) Phys Chem Chem Phys 5:333–341
5. Richmond G (2001) Annu Rev Phys Chem 52:357–389
6. Krisch MJ, Auria RD, Brown MA, Tobias DJ, Hemminger JC (2007) J Phys Chem C 111:13497–13509
7. Aloisio S, Hintze PE, Vaida V (2002) J Phys Chem A 106:363–370
8. Åstrand PO, Karlstrom G, Engdahl A, Nelander B (1995) J Chem Phys 102:3534–3554
9. Kumaresan R, Kolandaivel P (1995) Z Phys Chem 192:191
10. Priem D, Ha TK, Bauder A (2000) J Chem Phys 113:169–175
11. Rablen PR, Lockman JW, Jorgensen WL (1998) J Phys Chem A 102:3782–3797
12. Zhou ZY, Shi Y, Zhou XM (2004) J Phys Chem A 108:813–822
13. Raub S, Marian CM (2007) J Comput Chem 28:1503–1515
14. Wei DQ, Truchon JF, Sirois S, Salahub DR (2002) J Chem Phys 116:6028–6038
15. Akiya N, Savage PE (1998) AIChE J 44:405–415
16. Chelli R, Righini R, Califano S (2005) J Phys Chem B 109:17006–17013
17. Velardez G, Heully JL, Beswick JA, Daudey JP (1999) Phys Chem Commun 2:24–29
18. Lee C, Yang W, Parr RG (1998) Phys Rev B 37:785–789
19. Eichkorn K, Weigend F, Treutler O, Ahlrichs R (1997) Theor Chem Acc 97:119–124
20. Treutler O, Ahlrichs R (1995) J Chem Phys 102:346–354
21. Hehre WJ, Random L, Schleyer PvR, Pople JA (1986) Ab initio molecular orbital theory. Wiley, New York
22. Dunning TH Jr (1989) J Chem Phys 90:1007–1023
23. Woon DE, Dunning THJ (1993) J Chem Phys 98:1358–1365
24. Helgaker T, Jorgensen P, Olsen J (2000) Molecular electronic-structure theory, chap 15. Wiley, Chichester
25. Lii J-H (2002) Molecular mechanics (MM4). J Phys Chem A 106:8667–8679
26. Allinger NL, Zhu ZS, Chen K (1992) J Am Chem Soc 114:6120–6133
27. Halgren T (1996) J Comput Chem 17:490, 520, 553
28. Brooks BR, Bruccoleri RE, Olafson BD, States DJ, Swaminathan S, Karplus M (1983) J Comput Chem 4:187–217
29. Wang J, Cleplak P, Kollman PJ (2000) J Comput Chem 21:1049–1074
30. Jorgensen WL (2007) J Chem Theory Comput 3:1877–1885
31. Rick SW, Berne BJ (1996) J Am Chem Soc 118:672–679
32. Rick SW, Stuart SJ, Berne BJ (1994) J Chem Phys 101:6141–6156
33. Yang ZZ, Wu Y, Zhao DX (2004) J Chem Phys 120:2541–2557
34. Wu Y, Yang ZZ (2004) J Phys Chem A 108:7563–7576
35. Li X, Yang ZZ (2005) J Chem Phys 122:084514
36. Li X, Yang ZZ (2005) J Phys Chem A 109:4102–4111
37. Zhang Q, Yang ZZ (2005) Chem Phys Lett 403:242–247
38. Yang ZZ, Qian P (2006) J Chem Phys 125:064311

39. Yang ZZ, Zhang Q (2006) J Comput Chem 27:1–10
40. Guan QM, Yang ZZ (2007) J Theor Comput Chem 6:731–746
41. Cong Y, Yang ZZ (2000) Chem Phys Lett 316:324–329
42. Zhao DX, Liu C, Wang FF, Yu CY, Gong LD, Liu SB, Yang ZZ (2010) J Chem Theory Comput 6:795–804
43. Wang CS, Li SM, Yang ZZ (1998) J Mol Struct (Theochem) 430:191–199
44. Berendse HJC, Postma JPM, van Gunsteren WF, DiNola A, Haak JR (1984) J Chem Phys 81:3684–3690
45. Frisch MJ, Trucks GW, Schlegel HB, Scuseria GE, Robb MA, Cheeseman JR, Montgomery JAJ, Vreven T, Kudin KN, Burant JC, Millam JM, Iyengar SS, Tomasi J, Barone V, Mennucci B, Cossi M, Scalmani G, Rega N, Petersson GA, Nakatsuji H, Hada M, Ehara M, Toyota K, Fukuda R, Hasegawa J, Ishida M, Nakajima T, Honda Y, Kitao O, Nakai H, Klene M, Li X, Knox JE, Hratchian HP, Cross JB, Bakken V, Adamo C, Jaramillo J, Gomperts R, Stratmann RE, Yazyev O, Austin AJ, Cammi R, Pomelli C, Ochterski JW, Ayala PY, Morokuma K, Voth GA, Salvador P, Dannenberg JJ, Zakrzewski VG, Dapprich S, Daniels AD, Strain MC, Farkas O, Malick DK, Rabuck AD, Raghavachari K, Foresman JB, Ortiz JV, Cui Q, Baboul AG, Clifford S, Cioslowski J, Stefanov BB, Liu G, Liashenko A, Piskorz P, Komaromi I, Martin RL, Fox DJ, Keith T, Al-Laham MA, Peng CY, Nanayakkara A, Challacombe M, Gill PMW, Johnson B, Chen W, Wong MW, Gonzalez C, Pople JA (2004) GAUSSIAN-03. Gaussian, Inc., Wallingford, CT
46. Montgomery JA, Frisch MJ, Ochterski JW, Petersson GA (1999) J Chem Phys 110:2822–2827
47. Boys SF, Bernardi F (1970) Mol Phys 19:553–566
48. Hocking WH (1976) Z Naturforsch 31a:1113–1121
49. Bjarnov E, Hocking WH (1978) Z Naturforsch 33a:610–618
50. Kwei GH, Curl RFJ (1960) J Chem Phys 32:1592–1594
51. Estrin DA, Paglieri L, Corongiu G, Clementi E (1996) J Phys Chem 100:8701–8711
52. Pettersson M, Lundell J, Khriachtchev L, Rasanen M (1997) J Am Chem Soc 119:11715–11716
53. Frisch MJ, Head-Gordon M, Trucks GW, Foresman JB, Schlegel HB, Raghavachari K, Robb MA, Binkley JS, Gonzales C, DeFrees DJ, Fox DJ, Whiteside RA, Seeger R, Melius CF, Baker J, Martin RL, Kahn LR, Stewart JJP, Topiol S, Pople JA (1994) GAUSSIAN94. Gaussian, Pittsburgh, PA
54. Erlandsson G, Selen H (1958) Ark Fys 14:61
55. Dyke TR, Muenter JS (1973) J Chem Phys 59:3125–3127